Ultrasonics Sonochemistry 105 (2024) 106859

Contents lists available at ScienceDirect

Ultrasonics Sonochemistry

journal homepage: www.elsevier.com/locate/ultson

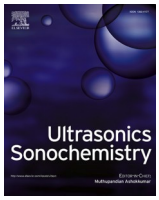

Mechanism study of aging oil demulsification and dehydration under ultrasonic irradiation

Jinbiao Gao [a,b], Jianjian Zhu [c], Qinghe Gao [d,*], Xiaoqing Zhao [a,b,*], Lanlan Yu [e], Jian Zhao [f], Fangchao Jia [f], Yunlong Wu [c], Limin Li [d], Jiashuai Guo [a]

[a] Earth Science College, Northeast Petroleum University, Daqing 163318, China
[b] National Key Laboratory of Continental Shale Oil, Northeast Petroleum University, Daqing 163318, China
[c] No.5 Oil Production Plant of Daqing Oilfield Co., Ltd., Daqing 163513, China
[d] Heilongjiang Provincial Key Laboratory of Oilfield Applied Chemistry and Technology, Daqing Normal University, Daqing 163712, China
[e] College of Chemistry and Chemical Engineering, Northeast Petroleum University, Daqing 163318, China
[f] Daqing Geophysical Exploration Company of BGP, CNPC, Daqing 163357, China

ARTICLE INFO

Keywords:
Ultrasound
Aging oil
Demulsification
Dehydration
Acoustic cavitation
Mechanism

ABSTRACT

With the tertiary oil recovery in the oilfield, the content of aging oil emulsion with high water content and complex components has become more prevalent, so it is crucial for aging oil to break the emulsification. In this paper, the experimental laws of water content are explored under the conditions of different transducer input powers through the ultrasonic reforming of aging oil, and the microscopic topography, particle size, components, etc. of oil samples before and after the irradiation of ultrasound are characterized through the microscopic analysis, particle size analysis and component analysis and other ways. The results show that the oil samples achieve the effect of demulsification and dehydration in the presence of ultrasonic cavitation effect, with a maximum dehydration rate of 98.24 %, and that the dehydration rate follows an "M−type" trend with the increase of power. The results of microscopic and particle size analyses demonstrate that ultrasonic irradiation destabilizes the oil–water interfacial membrane, and causes droplets of different sizes to collide, agglomerate, and settle. It was also observed that the droplets of the emulsion system are more evenly distributed and the intervals are increased. Furthermore, we hypothesize that ultrasound may be less irreversible in demulsification and dehydration of aging oil.

1. Introduction

The exploration, development, and effective utilization of fossil fuels such as oil and natural gas are of great strategic significance for sustainable development across the globe [1–3]. However, a major challenge in many oilfields, especially those entering intermediate and advanced stages of exploitation, is the rising moisture content in the produced fluid, which can even exceed 90 % [4,5]. To maintain the effective production of crude oil, numerous oilfields have employed chemical flooding oil recovery technology. Since the technology utilizes a large number of chemicals, it increases the concentration of heavy components, waxes, inorganic solid impurities, and metal ions in the crude oil, which leads to an intricate composition of the crude oil recovery fluid, and severe emulsification. Under the joint action of these substances over time, a layer of liquid-contaminated oil, known as the layer of oil aging, forms in the oil extraction fluid storage tanks, which is thickening, stable, and difficult for emulsification breaking [6,7].

As the aging oil continues to grow annually, and unprocessed discharge can cause environmental pollution and significant energy waste, it is a pressing issue to conduct dewatering and purification treatment of aging oil in oilfields [8–10]. Existing aging oil treatment methods, like the back blending treatment, electric field treatment, thermochemical dehydration, and biological emulsion breaking, have various drawbacks, including high demands for fresh crude oil, susceptibility to power tripping and collapse of the electric field phenomenon, challenges in the preparation of emulsion-breaking agent and the selection of strain, among others [11,12]. In contrast, the ultrasonic demulsification method offers a more novel, environmentally friendly

* Corresponding authors at: Earth Science College, Northeast Petroleum University, Daqing 163318, China (X. Zhao); Heilongjiang Provincial Key Laboratory of Oilfield Applied Chemistry and Technology, Daqing Normal University, Daqing 163712, China (Q. Goa).
E-mail addresses: gao5510113@163.com (Q. Gao), zhaoxiaoqing@nepu.edu.cn (X. Zhao).

https://doi.org/10.1016/j.ultsonch.2024.106859
Received 21 January 2024; Received in revised form 19 March 2024; Accepted 25 March 2024
Available online 26 March 2024

alternative with rapid efficacy, broad applicability, and no pollution to the formation. The technique could notably improve the physical properties of aging oil and realize the effect of dewatering when used in conjunction with other demulsification methods. Ultrasonic waves produce localized high temperatures, high pressures, shock waves, and micro-jets when radiating liquids, thus deriving cavitation, mechanical and thermal effects, which will reduce the surface tension and viscous force of the oil–water interface, then lead to the reduction of the stability of the oil–water interface, the separation of oil and water, the aggregation of water droplets, and ultimately the settling of the oil–water interface under the effect of gravity, thereby change the form of the existence of emulsions [13–15].

Despite its efficacy, no scholarly consensus has been reached on whether ultrasound alone is superior in terms of its effect on demulsification. Paczynska utilized a combination of ultrasound and heat at different frequencies to demulsify dirty oils and concluded that ultrasound alone was more effective than other approaches [16]. In contrast, in their comparison of the impact of ultrasonic and microbial methods on the stability of W/O emulsions, Vahdanikia et al. found that biosurfactants could reduce the surface tension of emulsions by about 15 %, and their demulsification effect surpassed that of ultrasonic method [17]. Amani et al. compared the effects of ultrasound, demulsifier, and centrifugation on demulsification and demonstrated that ultrasound was least effective in demulsification while centrifugation yielded the best results [18]. This view was echoed by Xu et al., who suggested that ultrasound alone might not be highly effective in demulsification [9].

Ultrasound can also be combined with other modalities for the study of demulsification and dehydration of emulsions, and scholars generally agree that the combined approach generates better outcomes. Yi et al. carried out crude oil demulsification experiments at different temperatures using ultrasound, chemical demulsification, and a combination of both, and the results showed that the combined approach was most effective in demulsification and that the dewatering rate of the emulsion increased with ultrasonic power and temperature, but remained unchanged with prolonged ultrasonic treatment time [19]. Similarly, Romanova et al. investigated the synergistic effects of ultrasound and nano-additives on emulsion destruction. Utilizing two different types of ultrasonic generators, their experiments examined the impact of the mode of ultrasonic irradiation, power, and time. The results demonstrated that efficient separation of emulsion could be achieved in a short period under optimal conditions, with a dehydration rate of 99 %, a substantial reduction in the concentration of mechanical impurities and iron sulfide, and an increase in the content of the oil phase [20].

In addition, there has been disagreement among scholars regarding the boundaries of ultrasonic demulsification and secondary emulsification of emulsions. Researchers at the Nanjing University of Technology advocated for a low power density in the demulsification of heavy oils and suggested that ultrasonic demulsification was inhibited at high power density and the ultrasonic irradiation time should not be controlled [21]. This view was supported by Yang et al., who observed that the first dewatering step increased and then decreased with rising ultrasonic power. They also noted that higher initial water content shortened the time required to break the emulsification, and with more profound efficacy [22]. Xu et al. also introduced the concept of an ultrasonic power critical value, where below this level, ultrasound acts as an emulsion breaker to enhance the dewatering rate of the emulsion with increasing power, and above this threshold, the separated oil and water would emulsify again [9]. Jianxin Qiao found that while the power of ultrasound had a minimal impact on demulsification, the effect of time was more significant. He revealed that the low-intensity steady-state ultrasonic cavitation increased the probability of water molecule channel formation by enhancing the collision rate of droplets to achieve the demulsification of heavy oil and that the water molecule channels could not be formed between droplets at high acoustic pressures, which resulted in the impediment of the demulsification process [23]. Luo et al. concluded that low-frequency ultrasound was particularly effective for separating emulsions with high viscosity and high interfacial strength and that the demulsification efficiency can be improved by increasing energy density to produce moderate cavitation [24]. **In contrast,** some scholars attributed the initial increase and subsequent decrease in the dehydration rate with growing sound intensity to the cavitation threshold. They argued that after reaching the cavitation threshold, ultrasound starts to exert an emulsifying effect on the liquid [11,25,26]. Referring to the cavitation threshold as the upper critical sound intensity, Wang et al. also noted that ultrasonic demulsification and dewatering should be carried out without ultrasonic cavitation effects and that the sound intensity should be controlled around the threshold [8].

In summary, the determination of the boundaries of demulsification and emulsification is of great significance to optimize the dehydration rate of aging oil and reveal the mechanism of aging oil dehydration and transformation under ultrasound. Here in this paper, we analyze the microscopic topography and particle size changes of oil samples under different conditions of ultrasonic transducer input electric power. The component contents of oil samples are determined by gas chromatography and column chromatography, and a comprehensive comparison reveals the mechanism of the water content variations of the aging oil. Finally, we conclude that demulsification and emulsification may coexist in the process of aging oil by ultrasonic irradiation, rather than a single presence. Meanwhile, we think that the cavitation effect can achieve demulsification and dehydration of aging oil, and therefore can be engineered to amplify the ultrasonic cavitation effect to enhance recovery of aging oil.

2. Method

2.1. Materials

The experimental sample used in this paper is a kind of aging oil from the Daqing oilfield in China, which has a dynamic viscosity of 15.086 mPa·s at 50 °C, and a standard density of 0.8646 g/cm^3. Other related parameters such as wax content and four-component content are shown in Table 1.

Additionally, the chemical reagents used in the experimental process include petroleum ether and anhydrous ethanol. Petroleum ether, a colorless and transparent liquid with a special odor and volatile properties, was acquired from Liaoning Quanrui Reagent Co., Ltd. with the implementation standard of GB/T 15894-2008 [27]. Anhydrous ethanol, also sourced from Liaoning Quanrui Reagent Co., Ltd., complies with GB/T 678-2002 standard [28], and it is a colorless, transparent volatile liquid with a relative molecular mass of 46.07 and a density of 0.789–0.791 g/ml at 20 °C.

2.2. Experimental process

2.2.1. Sample preparation

The experimental procedure is illustrated in Fig. 1. Firstly, 1.5 L aging oil samples were placed in 2 L beakers, which were then sealed and kept in a large static-sinking water bath (Changzhou Putian Instrument Manufacturing Co., Ltd., SY-1) at 80 °C for more than 3 h (to mitigate the history effect). The aging oil samples in the beaker were then homogenized using a high-speed homogenizer (Kinematica AG, Switzerland, PT 3100 D; 11,000 r/min for 2 mins). Finally, 50 ml of the homogenized sample was dispensed into 50 ml beakers and placed in a small thermostatic water bath (Gongyi Yuhua Instrument Co., Ltd., HH-S2) at 40 °C (to ensure a consistent initial temperature of the samples during ultrasonic irradiation) for spare use.

2.2.2. Ultrasonic irradiation

The frequency of the ultrasonic transducer (Hunan Lichen

Table 1
Component content of the original oil sample.

Name	Wax	Asphaltene	Resin	Saturated hydrocarbon	Aromatic hydrocarbon	Total hydrocarbon
Content (%)	25.19	0.28	16.79	82.11	7.76	89.87

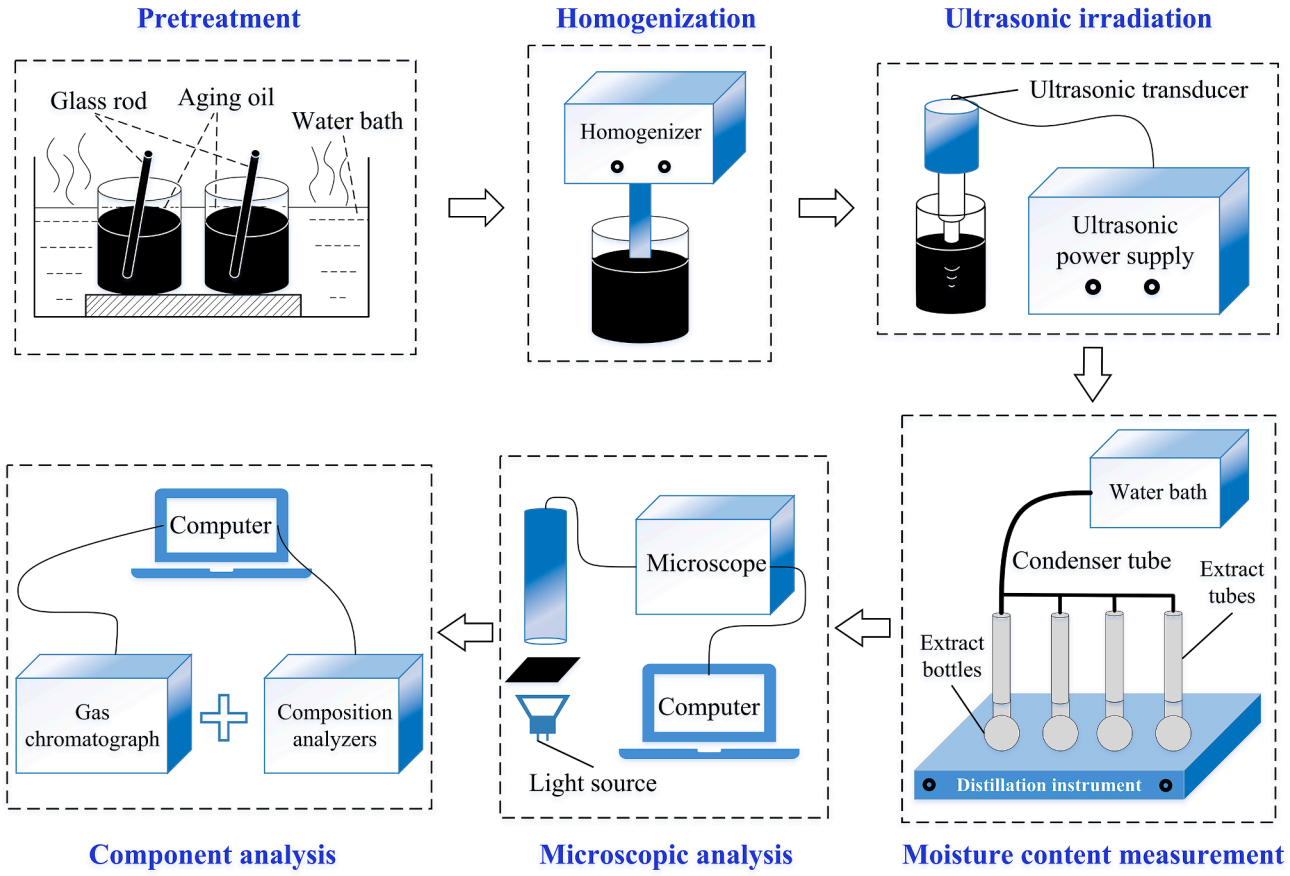

Fig. 1. The experimental flow chart.

Instrument Science and Technology Co., Ltd., LC-JY92-IIN) was about 20 kHz. A continuous mode of action was adopted. A variable amplitude rod probe was inserted into the sample to a depth of 1/3. The total electrical power (P) to the ultrasonic transducer is 650 W, and the actual treatment power was 20 %P, 40 %P, 60 %P, 80 %P, and 100 %P. To replicate the experimental laws, the ultrasonic irradiation time was set to be either 5 or 10 mins.

2.2.3. Moisture content measurement

The water content in the sample was measured by rapid magnetization distillation apparatus (Daqing Normal University, SYHS-12) according to the distillation method (GB/T 8929-2006) [29,30]. Firstly, we added the rotor and the appropriate amount of petroleum ether to the extraction bottle, and weighed the appropriate amount of the sample before and after ultrasonic irradiation in the extraction bottle with an electronic balance (Shimadzu Enterprise Management Co., Ltd., UW4200H), and the mass of the sample was recorded M. The extraction bottle, extraction tube, and condensation tube were then connected to ensure tight sealing. Next, the low-temperature thermostatic reaction bath and rapid magnetization distillation apparatus were turned on respectively, with continuous monitoring and observation for proper functionality of each place. Finally, after the automatic shutdown of the instrument and cooling of all parts to room temperature, the volume of water in the extraction tube was read V, and the formula of water content inside the oil sample φ is:

$$\varphi = \frac{m}{M} \times 100\% = \frac{\rho V}{M} \times 100\%$$

Where m indicates the mass of water obtained by distillation, ρ is 1 g/cm^3.

The dehydration rate ϕ is calculated by the formula:

$$\phi = \frac{\varphi_0 - \varphi}{\varphi_0} \times 100\%$$

Where φ_0 shows the water content of the initial oil sample, φ describes the water content of the oil sample after ultrasonic irradiation.

2.2.4. Microcosmic observation

To qualitatively analyze the effect of ultrasonic irradiation on the dehydration rate of aging oil, the microscopic morphology of different emulsions before and after ultrasonic irradiation was observed by microscopy (Shanghai Optical Instrument Factory No. 5, FRD-6C). Experimental samples for microscopic observation were first prepared using slides and coverslips. Then the objective lens and focal length were adjusted to facilitate clear observation of the microscopic images of the samples through external control software. Finally, the distribution of oil and water in the emulsion was obtained comparatively by changing the type of light source (fluorescent or halogen light). In this case, the magnification of the objective lens was 40 times, and the scale of the

acquired images was set uniformly at 50 μm.

2.2.5. Particle size analysis

The microscopic images of the oil samples before and after ultrasonic irradiation were imported into the particle size analysis software, and the diameter, cumulative number, area, and other information of the emulsion droplets were counted by the software to obtain the particle size changes of the aging oil samples under different experimental conditions. The resulting data were further used to quantitatively analyze the changes of the emulsion droplets of the aging oil before and after ultrasonic irradiation and to reveal the mechanism of the change in the water content in the aging oil from the viewpoint of the change in the particle size.

2.2.6. Component analysis

Different components and hydrocarbon distribution in the aging oil samples before and after ultrasonic irradiation were measured to analyze the relationship between the change in water content and the change in components and hydrocarbon content in the oil samples. This analysis aimed to elucidate the mechanism behind the water content change in aging oil from the perspective of the components and hydrocarbon changes. The specific measurement methods were as follows: Following the oil and gas industry standard SY/T 5119-2008 [31,32], the asphaltene content of different oil samples was determined by rod thin layer chromatography respectively. The wax content of different oil samples was calculated based on the standard SY/T 0537-2008 [33,34]. In addition, the distribution of carbon number in the oil samples was measured by gas chromatography (Agilent 7890A, SY/T 5779-2008 [35–37]).

3. Results and discussion

3.1. Variations in the moisture content of aging oil

As shown in Fig. 2, (a) and (b) present the variations of water content and dehydration rate of oil samples in relation to the electric power under varying ultrasonic irradiation times. The red and blue curves represent the ultrasonic irradiation time of 5 and 10 mins respectively. The star point indicates the water content and dehydration rate of the oil sample subjected to 5 mins of ultrasonic irradiation at 40 %P electric power, which is hypothesized based on the subsequent characterization results.

Overall, under different experimental conditions, the water content of the oil samples dropped from the initial 33.47 % to below 30 %. When the ultrasonic irradiation time was 5 mins, the water content of the oil samples showed a slight initial increase, decreased to its lowest point, and eventually rose again with the increment of electric power. The lowest water content was registered at 80 %P power, and an increase was observed once the power reached 100 %P. When the ultrasonic irradiation time was 10 mins, the water content in the oil samples showed a "W-type" trend in response to power changes, with the lowest point at 40 %P power and the highest point registered as the power reached 100 %P.

Conversely, the dehydration rate of the oil samples displayed an "M−type" pattern under both ultrasonic irradiation time conditions. Overall, the dehydration rate of oil samples exceeded 20 % under different experimental setups. Notably, at an ultrasonic irradiation time of 10 mins and electric power of 40 %P, the maximum dehydration rate of oil samples achieved was about 98.24 %.

3.2. The results of microstructure analysis

Fig. 3(a)-(f) depict the microscopic morphology of different oil samples observed under the conditions of different ultrasonic electric power at an ultrasonic irradiation time of 5 mins. The images are divided into two columns to represent the use of halogen light and fluorescence microscope light sources, respectively. In the halogen light images, the background aligns with the halogen light color, with the black color indicating the oil phase, and the bright color describing the aqueous phase. In contrast, in the fluorescence images, the background takes on the color of fluorescence, with black representing the aqueous phase and bright color the oil phase. The images of the two light sources can be compared to identify the type of emulsion droplets. For example, the emulsion droplets framed in the white dotted rectangular box of Fig. (a-1) have an oil film on the outside and water on the inside, i.e., they are water-in-oil type. This is further confirmed by the white dotted rectangular box of Fig. (a-2), where the black color in the interior signifies water, and the bright color on the outer edge indicates the oil phase [32,38,39].

The oil samples without ultrasonic treatment exhibit a complex internal composition, with water in the aging oil in the form of W/O dispersed in the continuous phase (oil). It could be seen in various types of emulsion droplets, such as the W/O, O/W/O, W/O/W/O, by the microscopic images. There are also small numbers of solid particles of impurities distributed in the oil phase. Water droplets in the aging oil are distributed in spherical and ellipsoidal forms, with particle sizes ranging from several microns to tens of microns. The emulsion droplets inside the initial oil sample are highly stable, which makes it difficult for large droplets to settle in the natural state, and for smaller-sized droplets, which are widely distributed in the emulsion, to aggregate due to strong

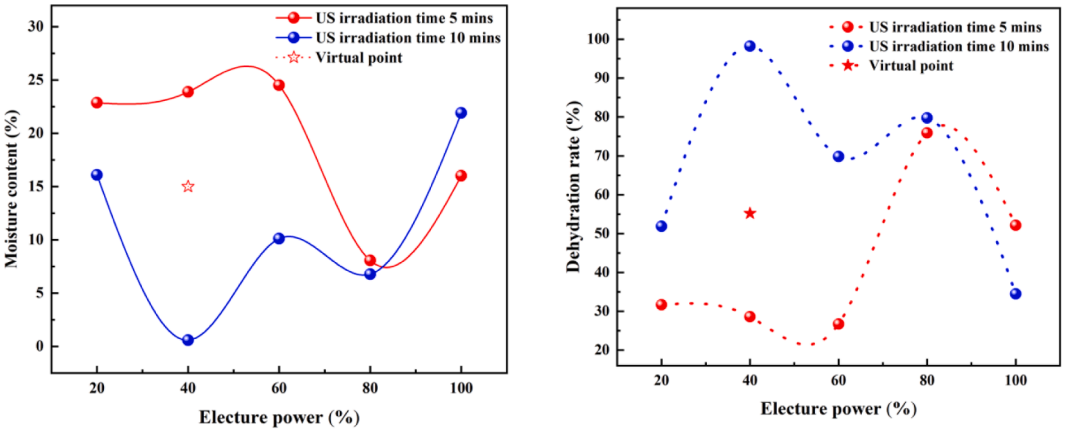

(a) The variations of water content (b) The variations of dehydration rate

Fig. 2. The results of water content and dehydration rate under different experimental conditions.

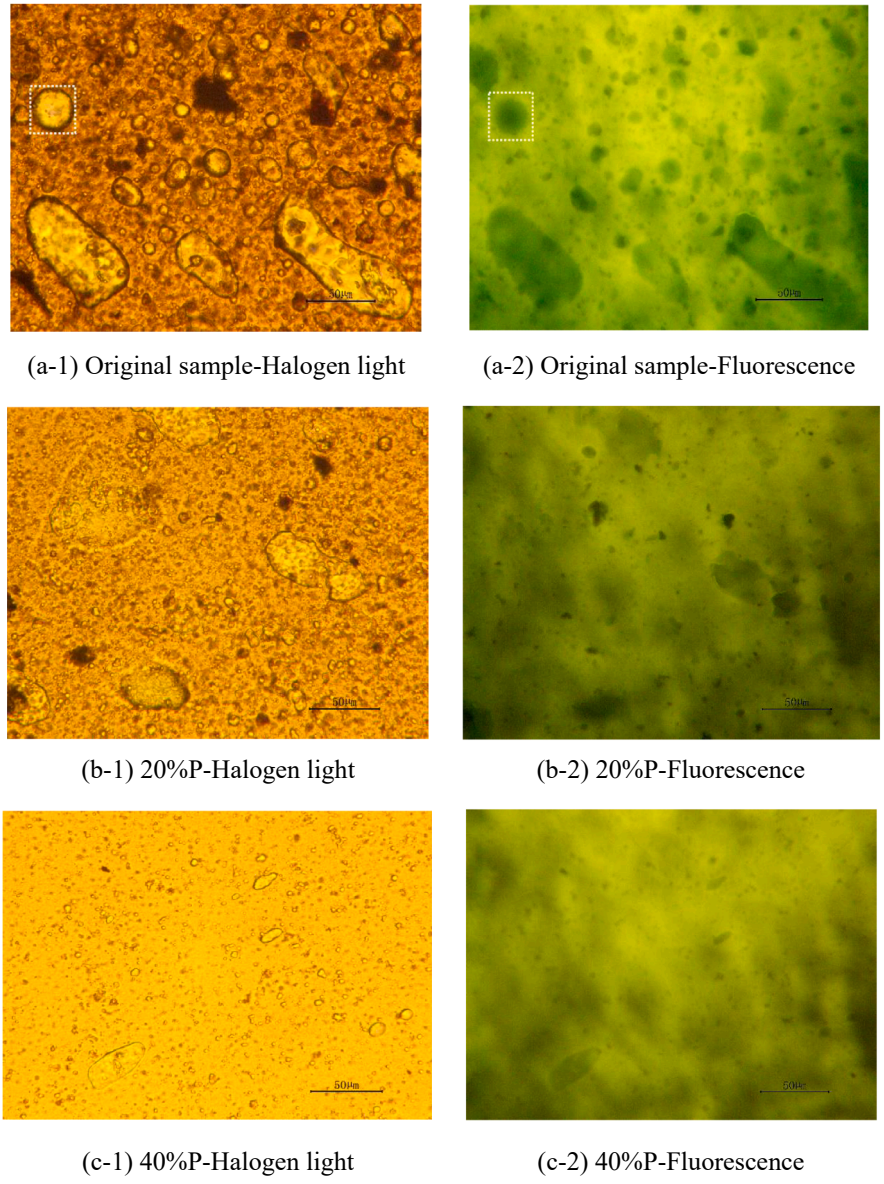

Fig. 3. Microscopic morphology of oil samples at 5 mins under ultrasonic irradiation.

oil–water interface stability. This stability is a significant factor in the challenges associated with demulsification and dehydration.

It is obvious from the microscopic images that the ultrasonic effect results in relatively fewer large-diameter droplets, a more homogeneous distribution, a relatively larger spacing, and a relative reduction in the complexity of the system after ultrasonic irradiation. There is also a significant difference in the distribution of droplets within the emulsion at different electrical powers.

As demonstrated in Fig. 4, (a) to (f) present the microscopic topography pictures of different oil samples obtained under varying electric powers with the halogen light source at an ultrasonic irradiation time of 5 mins.

Compared with the original oil samples, the microscopic system of the oil samples after 10 mins of ultrasonic irradiation became less complex, with fewer large-diameter droplets and larger inter-droplet intervals, which resulted in weaker inter-droplet interactions. The stability of the emulsions was also found to weaken due to the impact of intermolecular and interfacial tensions, which means that it was easier for emulsions to dehydrate.

Therefore, the analysis of the microscopic images of oil samples before and after ultrasound can provide qualitative insights: ultrasound disrupted the inherent equilibrium within the aging oil, the emulsion droplets within the oil samples underwent a more pronounced aggregation, and the large droplets settled under the effect of gravity. All this resulted in the reduction of the water content of the oil samples, which was consistent with the experimental laws obtained in *Section 3.1*. Besides, it could be observed that the emulsion droplets in some microscopic images were still in the process of aggregation/splitting.

3.3. Variations in the average diameter of water droplet

Figs. 5 and 6 quantitatively present the change laws of the average diameter of the emulsion droplets within different oil samples, at ultrasonic irradiation times of 5 and 10 mins, respectively. The bar graph illustrates the variations in average diameter with the change of the electric power (corresponding to the left axis), and the dotted line graph represents the change in the dehydration rate of the oil samples (aligned with the right axis).

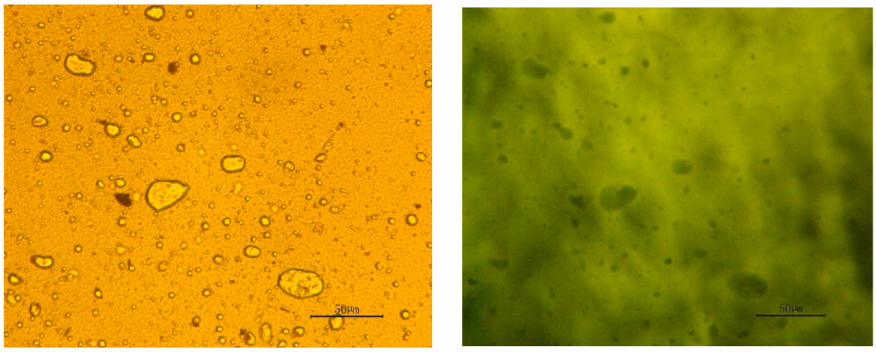

(d-1) 60%P-Halogen light (d-2) 60%P-Fluorescence

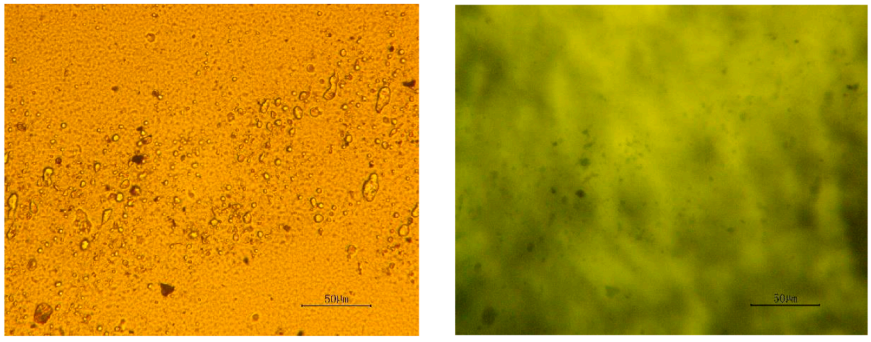

(e-1) 80%P-Halogen light (e-2) 80%P-Fluorescence

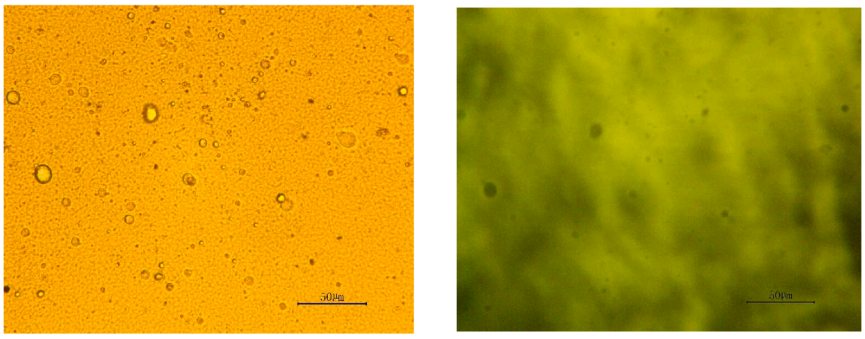

(f-1) 100%P-Halogen light (f-2) 100%P-Fluorescence

Fig. 3. (*continued*).

Two graphs show that, under different ultrasonic irradiation times, the average diameter of droplets displayed a wavy, "M−shaped" trend with increasing electric power. For the initial oil sample, the average diameter of the droplets was 0.40 μm, and after ultrasonic irradiation, the average diameter of the emulsion droplets was not less than 0.4 μm, with the largest reaching 0.78 μm. The increase in diameter means that the small-diameter droplets gradually converged to form larger-diameter droplets under the ultrasonic irradiation and the droplets would then be sunk under gravitational force after reaching a certain size, which was one of the main factors for the reduction in water content.

It was also observed that the changing rule of the average diameter of the droplets and the changing trend of the dehydration rate under different electric powers were consistent. Both had extreme values: at an ultrasonic irradiation time of 5 mins with 80 %P power, the dehydration rate of the oil samples peaked at 75.92 %, and at an ultrasonic irradiation time of 10 mins with 40 %P power, the dehydration rate of the oil samples reached an extreme value of 98.24 %. However, when the power was 100 %P, the average diameter of droplets was minimized under both ultrasonic irradiation times, and the dehydration rate was also reduced, which may suggest that the higher power and longer irradiation time did not lead to a higher dehydration rate of oil samples.

In addition, when comparing the variations in average diameter size of droplets under two ultrasonic irradiation times and the change rule of the dehydration rate of oil samples at the ultrasound irradiation time of 10 mins, it was observed that the moisture content measured at the ultrasound irradiation time of 5 mins with 40 %P power might have been subject to some error (possibly due to improper operation or errors in the readings in using the distillation method to measure water content). As such, the moisture content under this condition could be an extreme value and the actual value of moisture content is expected to fall between the values at the same condition when the power is 20 %–80 %P.

3.4. Component analysis

3.4.1. Gas chromatography analysis

The Fig. 7 demonstrate the results of gas chromatographic analysis under different experimental conditions. On the horizontal coordinate,

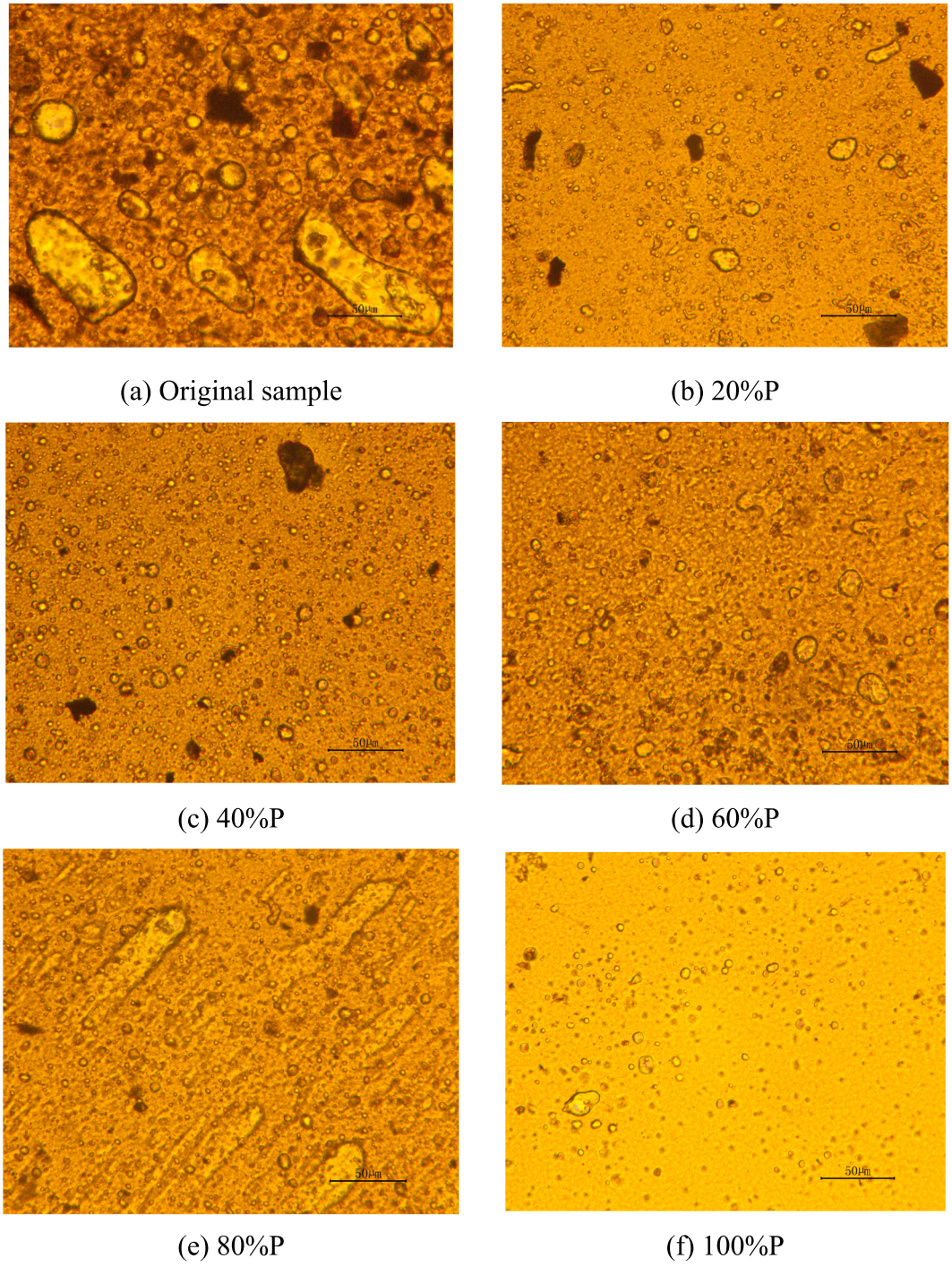

Fig. 4. Microscopic morphology of oil samples at 10 mins under ultrasonic irradiation (Halogen light).

"0" indicates the original oil samples without ultrasonic irradiation, while "1–5" and "6–10" indicate the increasing electric power levels at ultrasonic irradiation times of 5 and 10 mins, respectively. The colors of the bar graphs progress from lighter to darker, indicating the cumulative contents at carbon numbers <C10, C11-C20, C21-C40, and >C40, respectively.

Overall, the content of carbon number <C10 decreased and the content of C11-C20, C21-C40, >C40 increased in the oil samples after ultrasonic irradiation (in the majority of the oil samples). This indicates that compared with pre-ultrasound samples, the oil samples experienced a reduction in short carbon chains and an increase in long carbon chains after ultrasonic irradiation, i.e., the light component decreased, while the heavy component increased.

It is important to note that the experimental results in this section were measured appropriately one week after ultrasonic irradiation, and due to limited instrumentation, it was not possible to achieve complete synchronization. Hence, we hypothesize that shortly after ultrasonic irradiation, the light component content is elevated while the heavy component content is decreased, and that this change causes a decrease in the viscosity of the oil samples, thus decreasing the interfacial strength of the oil–water interface, and reducing the water content. After this critical period, the functional groups inside the oil sample will be reorganized, which resulted in increased carbon chains and heavy components. This growth enhanced dispersion between molecules, and

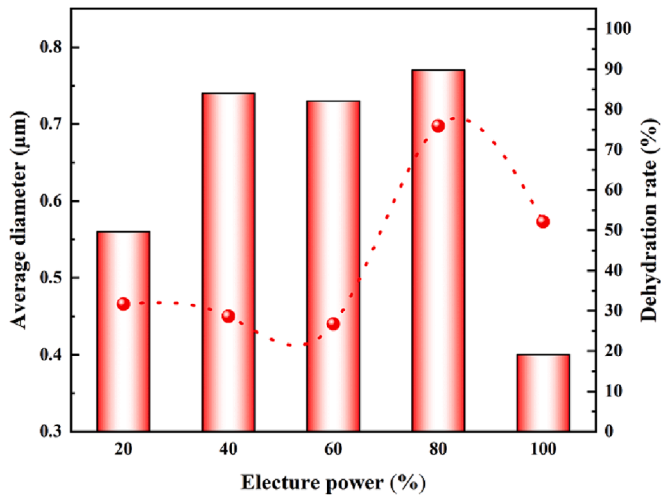

Fig. 5. Variations in the mean diameter of emulsion droplets at different powers during 5 mins of ultrasonic irradiation.

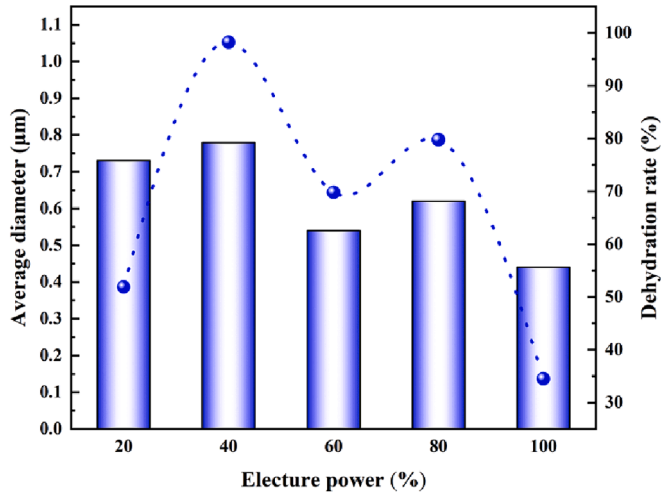

Fig. 6. Variations in the mean diameter of emulsion droplets at different powers during 10 mins of ultrasonic irradiation.

intermolecular forces, rendering it more difficult to break the emulsion. This also shows that ultrasonic demulsification may not be irreversible [40].

3.4.2. Asphaltene and wax content analysis

Fig. 8 displays the variations in asphaltene and wax content within the oil samples under the conditions of different powers and irradiation times. The horizontal axis, marked "0–10", follows the same notation as in the previous subsection. The red and blue bars indicate the variations in asphaltene and wax content in different oil samples, respectively.

The figure reveals that the asphaltene content in the original oil sample was about 0.28 %, and after ultrasonic irradiation, it underwent an upward trend, with the highest reaching 0.59 %. This increase is consistent with the law of the heightened content of the heavy component discussed in the part 3.4.1. The content and complex structure of asphaltene was an important factor for the viscosity of aging oil and the surface tension of the oil–water interface. An increase in asphaltene content tends to boost the stability of the emulsion, making demulsification and dehydration more challenging. This finding further raises questions regarding the irreversibility of ultrasound irradiation [40].

Pre-irradiation, the content of waxes in the oil samples was 25.19 %, and a reduction in wax content was spotted after ultrasonic irradiation in the majority of cases. This decrease has implications for the rheological properties of the emulsion, thereby affecting the stability of the emulsion in turn.

3.5. Mechanism analysis

One of the primary factors that contribute to the stability and difficulty in breaking aging oil emulsions is the stability of the oil–water interfacial membrane [41]. This membrane, a major barrier to droplet aggregation, has a large interfacial tension that reinforces the stability of the emulsion. The presence of asphaltenes, gums, waxes, and solid impurities further complicates the components and structure of emulsions, and high concentrations of cycloalkanes in macromolecules, such as asphaltenes and gums, result in high viscosity and frictional resistance, preventing the collision and aggregation of droplets and subsequently slowing down their sinking rate [42–44]. Asphaltenes can form a strong visco-elastic network at the oil–water interface, which serves as effective stabilizers for emulsions [45–47]. In addition, the presence of a small amount of colloid not only increases the solubility of asphaltene but also enhances their regular distribution at the interface, thus improving emulsion stability. The solid particles can be adsorbed on the interfacial membrane between oil and water to form a spatial barrier, thus minimizing the interactions between the interfaces and contributing to the enhancement of the stability of the emulsion [48].

The key to breaking the emulsification of aging oil is to reduce the interfacial tension of the oil–water interfacial membrane and destabilize the membrane so that the droplets can collide and agglomerate. Small droplets then gradually coalesce into large droplets, and settle, leading to achieve demulsification and dehydration [11].

Ultrasound generates intense cavitation, mechanical, and thermal effects in aging oil [49]. The three effects are a major factor for changes in the components, structure, and water content of aging oil.

Some researchers argued that ultrasonic demulsification should be conducted when the acoustic pressure is below the cavitation threshold, and that exceeding it could lead to secondary emulsification of the emulsion [8,9,11,25,26]. **However, our findings in this study suggest otherwise.** The experiments in this paper, conducted under the condition of the cavitation effect, demonstrated that the water content in the oil samples under each condition was lower than that in the original oil samples. Based on the experimental law of the "M−type" dehydration rate obtained in this paper and the analysis of the microscopic topography, the authors speculate that the demulsification and emulsification of the emulsion induced by ultrasound are not entirely separated, i.e., the two effects may exist simultaneously. This co-existence could be influenced by a cumulative effect of the size of acoustic energy and the ultrasonic duration: when the cumulative effect favors demulsification over emulsification, an increase in the dehydration rate of the emulsion is observed, and conversely, when the cumulative effect leans towards emulsification, a decrease in the dehydration rate of the emulsion is registered.

The schematic diagram of the mechanism of demulsification under ultrasonic irradiation is shown in Fig. 9. The ultrasonic cavitation effect, generated during ultrasonic irradiation, produces localized high temperature, high pressure, shock wave, and micro-jet within the liquid [50,51]. This enormous energy will significantly damage the interfacial membrane of the emulsion droplets suspended in the aging oil. The existence of thermal effects will reduce the viscosity of the emulsion, which in turn weakens the interfacial strength of the oil–water interfacial membrane, and causes the membrane to rupture. In addition, the mechanical effect and the presence of acoustic energy flow [52] can produce violent oscillations in the emulsion system, resulting in varying relative vibration speeds for different droplets, and thereby promoting the collision of water droplets and agglomeration. According to Stokes' formula [53], when the volume of agglomerated droplets reaches a certain value, they settle under the influence of gravity, thus reducing the water content of the emulsion. However, the increase of electric

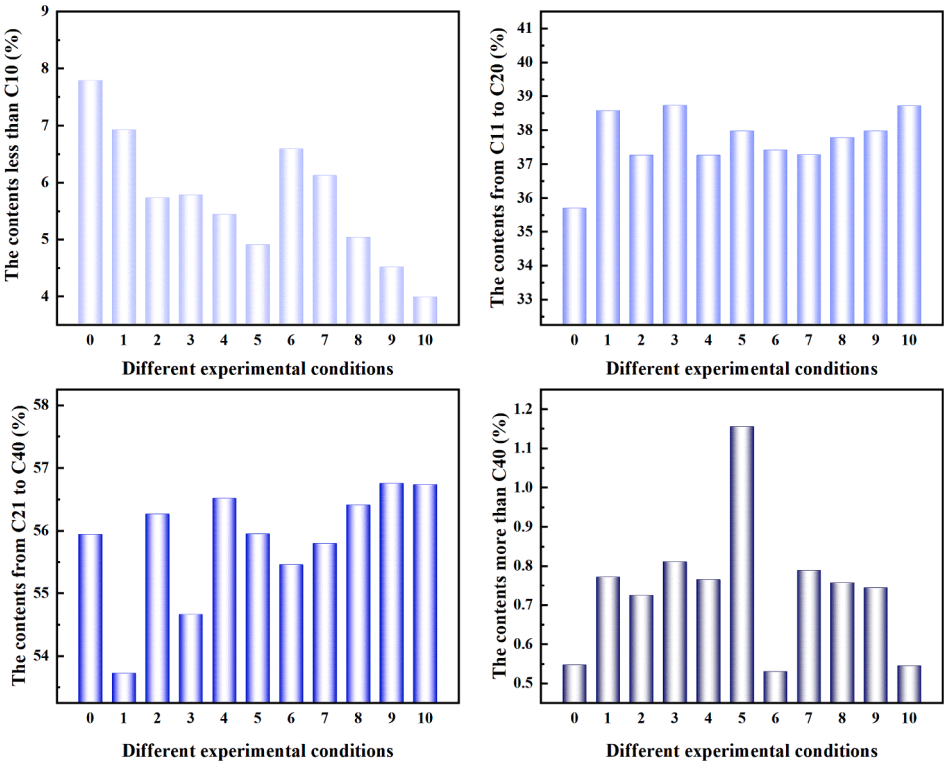

Fig. 7. The analysis results of gas chromatographic under different ultrasonic electric power and irradiation time.

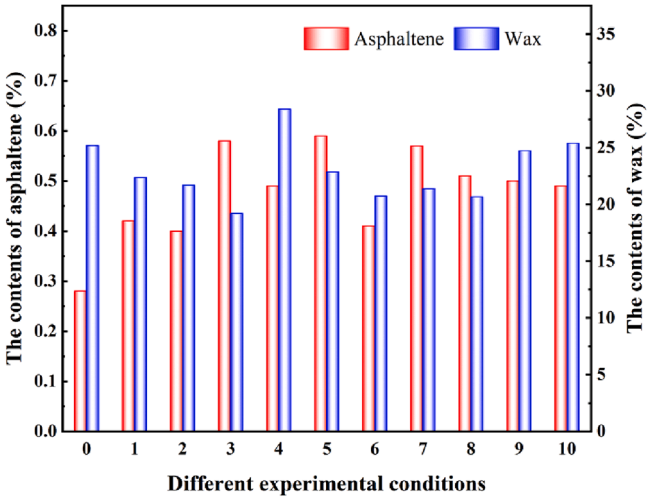

Fig. 8. Variation of asphaltene and wax content under different ultrasonic electric power and irradiation time.

power and acoustic energy affects the stability of the oil–water interface, and thus causes different intensities of demulsification and emulsification effects in oil samples varies, resulting in "M−type" changes in the water content of the oil samples.

It was also found that the content of heavy components in the oil samples increased after some time under ultrasonic irradiation, which means that the viscosity of the emulsion increased after the water content was reduced, and the increase in adhesion will enhance the stability of the oil–water interface. Moreover, the figures of microscopic morphology showed that the size of the emulsion droplets decreased, and the intervals increased post-ultrasonic irradiation, which may indicate enhanced stability of the emulsion despite reduced water content of the emulsion after the ultrasonic irradiation. This illustrates that the effects of ultrasound action are not irreversible.

4. Conclusion and prospect

The exact mechanisms of ultrasonic aging oil demulsification and reforming remain elusive. To uncover its underlying mechanisms, the research employed microscopic topography analysis, particle size analysis, component analysis, and other methods to characterize the water content, microscopic topography, particle size, components, etc. of the aging oil before and after ultrasonic irradiation. The key conclusions are as follows:

(1) The cavitation effect can also be achieved for the decrease of water content. The demulsification and emulsification may be carried out at the same time under ultrasonic irradiation. (2) At ultrasonic irradiation times of 5 or 10 mins, the dehydration rate of the oil samples displays an "M−type" trend with rising ultrasonic electric power, indicating that both low and high levels of electric power are not effective for the dewatering of the oil samples. (3) The ultrasonic irradiation can produce intense cavitation, mechanical, and thermal effects. The combination of the three effects can change the internal structure of the aging oil and disrupt the stability of the oil–water interfacial membrane, resulting in the collision and agglomeration of water droplets. Consequently, the droplets and intervals become larger, and ultimately settle, thus lowering the water content in the emulsion.

Looking ahead, future research should investigate the roles of demulsification and emulsification on the dehydration rate during ultrasonic irradiation of aging oil through optical and chemical means. In addition, employing the cavitation noise method to examine the relationship between cavitation intensity and the emulsification and dehydration of aging oil, and incorporating theories of vacuolar dynamics and acoustic free radicals in research will be significant in understanding the acoustic mechanisms in ultrasonic demulsification and reforming of aging oil.

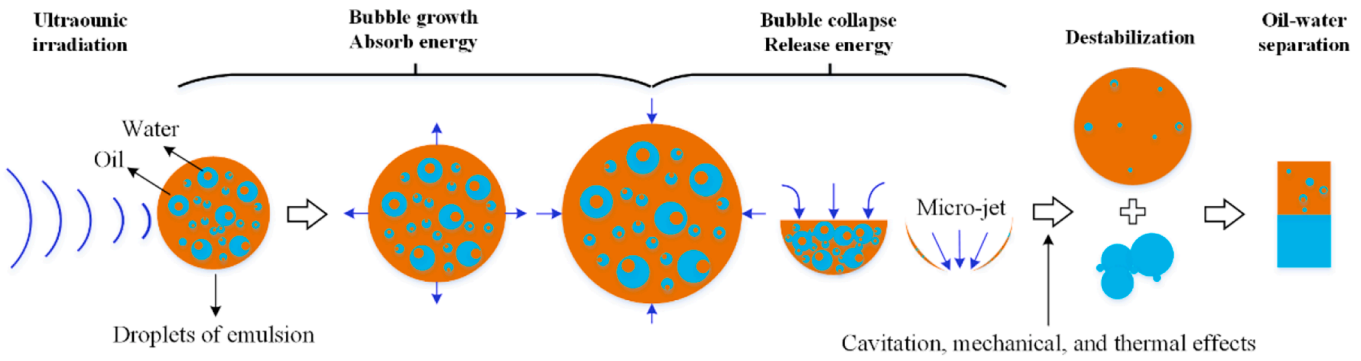

Fig. 9. Schematic diagram of the mechanism of demulsification under ultrasonic irradiation.

CRediT authorship contribution statement

Jinbiao Gao: Writing – review & editing, Writing – original draft, Software, Project administration, Methodology, Formal analysis, Data curation. **Jianjian Zhu:** Methodology, Formal analysis, Data curation. **Qinghe Gao:** Supervision, Investigation, Funding acquisition. **Xiaoqing Zhao:** Writing – review & editing, Supervision, Investigation. **Lanlan Yu:** Methodology. **Jian Zhao:** Data curation. **Fangchao Jia:** Formal analysis. **Yunlong Wu:** Data curation. **Limin Li:** Data curation. **Jiashuai Guo:** Data curation.

Declaration of competing interest

The authors declare that they have no known competing financial interests or personal relationships that could have appeared to influence the work reported in this paper.

Acknowledgments

This work is supported by the Natural Science Foundation of Heilongjiang Province (No. LH2021B001). Thanks go to Mr. Jingbo Zhao, Zhonggui Luo, Haifeng Wang (Daqing Normal University) for their help in the experimental characterizations.

References

[1] J. Gao, X. Shen, X. Mo, et al., Study on the real-time variation laws and mechanism of oil sample viscosity during ultrasonic irradiation[J], Ultrason. Sonochem. 98 (2023) 106460.
[2] Y. Ji, X. He, H. Chen, et al., Acoustic fields for monopole logging while drilling with an eccentric collar[J], Geophysics 86 (2) (2021) D43–D63.
[3] M. Jiang, X. Fu, Z. Wang, An experimental investigation of the characteristics of cataclastic bands in high-porosity sandstones[J], Geol. Soc. Am. Bull. (2024) B36801.1.
[4] M. Song, The stability analysis and synthetical treatments study of aging oil[D], China University of Petroleum (East China), Shandong, 2014.
[5] Y. Wang, X. Han, J. Li, et al., Review on oil displacement technologies of enhanced oil recovery: State-of-the-art and outlook[J], Energy Fuel 37 (4) (2023) 2539–2568.
[6] W.L. Zheng, R.S. Pang, Experimental study on aging oil dehydration technology optimization in Yushulin oilfield[J], Adv. Mat. Res. 393–395 (2011) 746–749.
[7] B. Chen, Study on the synthesis and dehydration process of high-efficiency demulsifiers for aged oil in Tuha Oilfield[D], Northeast Petroleum University, Heilongjiang, 2023.
[8] Z. Wang, S. Gu, L. Zhou, Research on the static experiment of super heavy crude oil demulsification and dehydration using ultrasonic wave and audible sound wave at high temperatures[J], Ultrason. Sonochem. 40 (2018) 1014–1020.
[9] X. Xu, D. Cao, J. Liu, et al., Research on ultrasound-assisted demulsification/dehydration for crude oil[J/OL], Ultrason. Sonochem. 57 (2019) 185–192.
[10] J. Ma, M. Yao, Y. Yang, et al., Comprehensive review on stability and demulsification of unconventional heavy oil-water emulsions[J], J. Mol. Liq. 350 (2022) 118510.
[11] Z. Fajun, T. Zhexi, Y. Zhongqi, et al., Research status and analysis of stabilization mechanisms and demulsification methods of heavy oil emulsions[J], Energy Sci. Eng. 8 (12) (2020) 4158–4177.
[12] B. Hen, H. Chen, H. Liang, et al., Research progress of aging oil dehydration treatment process[J], Desalin. Water Treat. 219 (2021) 1–10.
[13] P. Wu, X. Wang, W. Lin, et al., Acoustic characterization of cavitation intensity: A review[J], Ultrason. Sonochem. 82 (2022) 105878.
[14] Y. Tao, P. Wu, Y. Dai, et al., Bridge between mass transfer behavior and properties of bubbles under two-stage ultrasound-assisted physisorption of polyphenols using macroporous resin[J], Chem. Eng. J. 436 (2022) 135158.
[15] S. Lin, J. Zhang, D. Stekel, et al., The food matrix properties influence the antibacterial effectiveness of photodynamic and sonodynamic treatments[J], Innov. Food Sci. Emerg. Technol. 93 (2024) 103630.
[16] L.B. Paczynska, Demulsification of petroleum emulsions with ultrasound[J], Erdoel Erdgas Kohle 105 (7) (1989) 317–318.
[17] N. Vahdanikia, H. Divandari, A. Hemmati-Sarapardeh, et al., Integrating new emerging technologies for enhanced oil recovery: Ultrasonic, microorganism, and emulsion[J], J. Pet. Sci. Eng. 192 (2020) 107229.
[18] M.I. Amani, M.A. Ghani, et al., An experimental study on the application of ultrasonic technology for demulsifying crude oil and water emulsions[J], J. Petrol. Environ. Biotechnol. 8 (3) (2017).
[19] M. Yi, J. Huang, L. Wang, Research on crude oil demulsification using the combined method of ultrasound and chemical demulsifier[J], J. Chem. (2017) 9147926.
[20] Y.N. Romanova, T.A. Maryutina, N.S. Musina, et al., Application of ultrasonic treatment for demulsification of stable water-in-oil emulsions[J], J. Pet. Sci. Eng. 209 (2022) 109977.
[21] Y. Cai, Study of demulsification, dehydration and desalination of static crude oil emulsion by ultrasound[D], Nanjing University of Technology, Jiangsu, 2005.
[22] X. Yang, W. Tan, X. Tan, Demulsification of crude oil emulsion via ultrasonic chemical method[J], Pet. Sci. Technol. 27 (17) (2009) 2010–2020.
[23] J. Qiao, Research on mechanism of heavy oil emulsification/demulsification and upgrading process by power ultrasonics[D], Harbin Institute of Technology, Heilongjiang, 2022.
[24] X. Luo, H. Gong, H. Yin, et al., Optimization of acoustic parameters for ultrasonic separation of emulsions with different physical properties[J], Ultrason. Sonochem. 68 (2020) 105221.
[25] G.R. Check, D. Mowla, Theoretical and experimental investigation of desalting and dehydration of crude oil by assistance of ultrasonic irradiation[J], Ultrason. Sonochem. 20 (1) (2013) 378–385.
[26] M.F. Pedrotti, M.S.P. Enders, L.S.F. Pereira, et al., Intensification of ultrasonic-assisted crude oil demulsification based on acoustic field distribution data[J], Ultrason. Sonochem. 40 (2018) 53–59.
[27] Y. Hao, Y. Huang, H. Cheng, Chemical Reagent-Petroleum Ether: GB/T 15894[S], Standards Press of China, Beijing, 2008.
[28] J. Sun, L. Li, Chemical Reagent-Ethanol: GB/T 678[S], Standards Press of China, Beijing, 2002.
[29] Y. Bo, J. Li, Crude Petroleum-Determination of Water-Distillation Method: GB/T 8929[S], Standards Press of China, Beijing, 2006.
[30] J. Zhang, X.J. Wang, Q. Liang, et al., Demulsification law of polyether demulsifier for W/O crude oil emulsion containing hydrophobically modified polyacrylamide in water[J], J. Mol. Liq. 394 (2024) 123805.
[31] L. Zheng, H. Wang, J. Meng, et al., Analytical Method of Hydrocarbons in Petroleum and Sediment By Gas Chromatography: GB/T 5119[S], Standards Press of China, Beijing, 2008.
[32] B. Tania, S. Marzieh, M. Ali, et al., Eco-friendly and efficient demulsification by chitosan biopolymer modified with titanium dioxide nanohybrid on carbonaceous substrates in (W/O) emulsions of crude oil [J], J. Sol-Gel Sci. Technol. 104 (1) (2022) 211–224.
[33] Y. Lin, Q. Song, Y. Liu, The Test Method of Wax Content in Crude Oil: SY/T 0537 [S], Standards Press of China, Beijing, 2008.
[34] Z.C. Niu, Y.S. Wang, Z. Li, et al., Analysis of the spatial distribution Characteristics of crude oils with different freezing points and the genetic mechanism of high-freezing-point crude oils in the Dongying Sag[J], ACS Omega 8 (38) (2023) 35093–35106.
[35] T. Xiao, L. Li, J. Zhang, et al., Analytical Method of Hydrocarbons in Petroleum and Sediment by Gas Chromatography: SY/T 5779[S], Standards Press of China, Beijing, 2008.
[36] G. Bai, C. Ma, X. Chen, Phytosterols in edible oil: Distribution, analysis and variation during processing [J], Grain Oil Sci. Technol. 4 (1) (2021) 33–44.

[37] K.F. Fan, S. Li, W.D. Li, Experimental study on the wax deposit properties in the radial direction in crude oil pipeline: wax precipitation, carbon number distribution[J], Pet. Sci. Technol. 40 (19) (2022) 2319–2335.
[38] E. Malek, D.V. Auke, R. Dérick, Demulsification of water-in-oil emulsions stabilized with glycerol monostearate crystals[J], J. Colloid Interface Sci. 636 (2022) 637–645.
[39] M.S.A. Mahmood, O.E. Abdelrahman, A.A. Hamad, et al., New amphiphilic ionic liquids for the demulsification of water-in-heavy crude oil emulsion[J], Molecules 27 (10) (2022) 3238.
[40] Z. Tian, Research on stability and demulsification and dehydration mechanism of heavy oil emulsion in Liaohe oilfield[D], Northeast Petroleum University, Heilongjiang, 2020.
[41] T. Strøm-Kristiansen, A. Lewis, P.S. Daling, et al., Heat and chemical treatment of mechanically recovered W/O emulsions[J], Spill Sci. Technol. Bull. 2 (2–3) (1995) 133–141.
[42] J.B.V.S. Ramalho, F.C. Lechuga, E.F. Lucas, Effect of the structure of commercial poly (ethylene oxide-b-propylene oxide) demulsifier bases on the demulsification of water-in-crude oil emulsions: Elucidation of the demulsification mechanism[J], Quim. Nova 33 (8) (2010) 1664–1670.
[43] D. Nguyen, V. Balsamo, J. Phan, Effect of diluents and asphaltenes on interfacial properties and SAGD emulsion stability: Interfacial rheology and wettability[J], Energy Fuel 28 (3) (2014) 1641–1651.
[44] P. Tchoukov, F. Yang, Z. Xu, et al., Role of asphaltenes in stabilizing thin liquid emulsion films[J], Langmuir 30 (11) (2014) 3024–3033.
[45] J.D. McLean, P.K. Kilpatrick, Effects of asphaltene aggregation in model heptane-toluene mixtures on stability of water-in-oil emulsions[J], J. Colloid Interface Sci. 196 (1) (1997) 23–34.
[46] M.F. Ali, M.H. Alqam, The role of asphaltenes, resins and other solids in the stabilization of water in oil emulsions and its effects on oil production in Saudi oil fields[J], Fuel 79 (2000) 1309–1316.
[47] P. KILPATRICK, P. MATTHEW SPIECKER. Asphaltene Emulsions[M]//SJÖBLOM J. Encyclopedic Handbook of Emulsion Technology. CRC Press, 2001: 707-730.
[48] Y. Yan, J.H. Masliyah, Solids-stabilized oil-in-water emulsions: scavenging of emulsion droplets by fresh oil addition[J], Colloids Surf. A Physicochem. Eng. Asp. 75 (1993) 123–132.
[49] J. Gao, C. Li, D. Xu, et al., The mechanism of ultrasonic irradiation effect on viscosity variations of heavy crude oil[J], Ultrason. Sonochem. 81 (2021) 105842.
[50] J. Gao, P. Wu, C. Li, et al., Influence and mechanism study of ultrasonic electric power input on heavy oil viscosity[J], Energies 16 (1) (2022) 79.
[51] Y. Zang, Radial and translational motions of a gas bubble in a Gaussian standing wave field[J], Ultrason. Sonochem. 101 (2023) 106712.
[52] F.G. Antes, L.O. Diehl, J.S.F. Pereira, et al., Effect of ultrasonic frequency on separation of water from heavy crude oil emulsion using ultrasonic baths[J], Ultrason. Sonochem. 35 (2017) 541–546.
[53] M.A. Mehrnia, S.M. Jafari, B.S. Makhmal-Zadeh, et al., Rheological and release properties of double nano-emulsions containing crocin prepared with Angum gum, Arabic gum and whey protein[J], Food Hydrocoll. 66 (2017) 259–267.